https://doi.org/10.5194/egusphere-2023-1477
Preprint. Discussion started: 7 September 2023

Hector V3.1.1: functionality and performance of a reduced-complexity climate model

Kalyn Dorheim[1], Skylar Gering[2], Robert Gieseke[3], Corinne Hartin[4], Leeya Pressburger[1], Alexey N. Shiklomanov[5], Steven J. Smith[1], Claudia Tebaldi[1], Dawn Woodard[1,6], Ben Bond-Lamberty[1]

[1]University Joint Global Change Research Institute, Pacific Northwest National Laboratory, 5825 University Research Ct. #3500, College Park, MD 20740 USA
[2] California Institute of Technology 1200 E California Blvd, Pasadena, CA 91125 USA
[3] Independent Researcher, Potsdam, Germany
[4] Climate Change Division, Office of Atmospheric Protection, U.S. Environmental Protection Agency, Washington, DC, USA
[5] NASA Goddard Space Flight Center, 8800 Greenbelt Rd., Greenbelt, MD, 20771 USA
[6] Natural Resources Defense Council, 1152 15th St NW #300, Washington, DC 20005

Correspondence to: Kalyn Dorheim (kalyn.dorheim@pnnl.gov)

Abstract. Hector, an open-source reduced complexity climate-carbon cycle model. Hector is a computationally efficient source of climate information, capable of completing a run in a fraction of a second. Hector models critical Earth system processes on a global and annual basis. Here we present an updated version of the model, Hector V3.1.1 (hereafter Hector V3). In this manuscript, we document Hector's new features, and implementation of new science (e.g., radiative forcing calculations, carbon cycle, etc.). Hector V3 results are in good agreement with historical observations of CO_2 concentrations and global mean surface temperature, and its future temperature projections are consistent with more complex Earth System Model output data from the Sixth Coupled Model Intercomparison Project. We document that Hector V3 is a flexible, performant, and robust simulator of contemporary and 21st-century global climate, and in closing, discuss future areas of improvement and research with respect to the model's scientific, stakeholder, and educational priorities.

1 Introduction

Reduced complexity climate models (RCMs) fill a critical role within the diverse climate modeling landscape (Sarofim et al., 2021). By operating at lower resolutions with strategically simpler representations of large-scale climate processes and dynamics in contrast to coupled Earth System Models (ESMs), RCMs are computationally-efficient sources of future climate projections, able to produce large ensembles of results, often exploring key uncertainties, at a fraction of the computational cost of a single ESM run (Kawamiya et al., 2020). For this reason, RCMs such as Hector, MAGICC, FaIR, and the other Reduced Complexity Intercomparison Project (RCMIP) participating models (Nicholls et al., 2020, 2021; Meinshausen et al., 2011; Smith et al., 2018) have been coupled with socioeconomic models (Calvin et al., 2019a; Hartin et al., 2023); used to study climate-carbon interactions and feedbacks (Woodard et al., 2021); supported the assessment of key quantities like global

https://doi.org/10.5194/egusphere-2023-1477
Preprint. Discussion started: 7 September 2023

temperature and the carbon budget in various Intergovernmental Panel on Climate Change (IPCC) reports (Clarke, 2014; Smith et al., 2021; Forster et al., 2021); and other applications. Here we focus on one such RCM, Hector.

First described by (Hartin et al., 2015), Hector is a globally resolved carbon-climate model with explicit terrestrial and ocean carbon cycles as well as active surface ocean chemistry. As a stand-alone climate model, Hector has been used in a variety of other research projects (Woodard et al., 2021; Dorheim et al., 2020; Schwarber et al., 2019; Vega-Westhoff et al., 2019; Pressburger et al., 2023) and participated in the first two phases of RCMIP (Nicholls et al., 2020, 2021). In addition, since 2015, Hector has been the climate component of the Global Change Analysis Model (GCAM) (Calvin et al., 2019b) and used to explore the feedback from hydrofluorocarbon emissions from future changes in heating and cooling degree days (Hartin et al., 2021) and to explore how carbon dioxide (CO_2) removal technologies may impact the energy-water-land system (Fuhrman et al., 2023). Since its initial release, model development of Hector has continued in order to reflect the advances made within the climate science and open-source software research communities.

The objective of this paper is to document the latest version of Hector. To begin, we provide a brief overview of the model before focusing on the major changes and upgrades that have been made since Hector V1. Next, we compare Hector V3 results with observations and ESM output to examine model performance. Finally, we discuss future areas of improvement for the model in the context of its goals of accuracy, performance, and broad accessibility.

2 Methods

2.1 Model Description

The first version of Hector (V1) was described in detail by Hartin et al. (2015). Here we first summarize the model's unchanged functionality, without reproducing all of the detailed equations given by Hartin et al. (2015). Hector is a self-contained object-oriented model implemented in C++ with a modular, flexible design. While Hector produces annual output, its adaptive-time solver is capable of operating at a higher frequency to help address issues with numerical instability.

In its default configuration, all Hector runs begin after "spinup" (Thornton and Rosenbloom, 2005), in which the model runs until all carbon pools are in equilibrium; this typically requires ~300 years using the default model parametrization. After the spinup phase is complete, the main Hector run begins (Hartin et al., 2015). A Hector run can either be "free-running" or "constrained." By default, the model is free-running, meaning that its behavior is determined by the time series of emissions and other inputs. Whereas during a *constrained* run, the model is forced to match one or more user-prescribed time series, e.g., CO_2 concentrations or temperature (see § 2.2.5 below).

https://doi.org/10.5194/egusphere-2023-1477
Preprint. Discussion started: 7 September 2023

Free-running Hector, the default, uses time series from 37 different emission species and 3 exogenous radiative forcers. The emissions are passed into Hector's well-mixed global atmosphere. These input emissions fall into two categories (§ 2.2.3). The first category is emissions that accumulate as (GHG) concentrations. The GHG concentrations for non-CO_2, (nitrous oxide (N_2O), methane (CH_4), and 26 halocarbons) are calculated using equations that portray a simplified relationship between emissions and concentrations (see equations 15, 16, 18, 24, and 31 of Hartin et al. (2015)). The atmospheric CO_2 concentrations are determined in part by the anthropogenic CO_2 emissions (read in as an input) and also by the behavior of Hector's terrestrial and ocean carbon cycle components (**Figure 1**). The second category is emissions that impact Hector's radiative forcing budget, such as carbon monoxide (CO), black carbon (BC), organic carbon (OC), sulfur dioxide (SO_2), and ammonia (NH_3). These emissions are used in equations (see supplement) that determine aerosol and other forcings. Reactive gas emissions impact global tropospheric ozone (O_3) forcing and the lifetime of methane.

After the radiative forcing effects from all the GHGs have been determined, the total radiative forcing is calculated. The total radiative forcing is the sum of the forcing effects of all of Hector's atmospheric gases, aerosols, and other externally defined forcing inputs (e.g., volcanic forcing and albedo).

Total radiative forcing is then used to simulate temperature change. Hector's temperature component (Vega-Westhoff et al., 2019) is an implementation of the Diffusion Ocean Energy balance CLIMate model (DOECLIM, (Tanaka et al., 2007; Kriegler, 2005). DOECLIM is a 1-D pure diffusion ocean model used to calculate changes in tropospheric temperature over ocean/land, sea surface temperature, and within the ocean mixed layer. The sea surface and land surface temperatures from DOECLIM are then used by Hector's ocean and land carbon cycles to calculate the carbon fluxes at the next time step (§ 2.2.2). Hector's GMST is the area-weighted average of land surface and ocean surface temperatures.

2.2 Changes Since V1

A number of significant architectural, software, and scientific developments have been implemented since the V1 release and documentation manuscript (Hartin et al., 2015). We start by documenting these software changes before discussing other changes and new features affecting Hector's carbon cycle, radiative forcing, temperature calculations, and constrained mode capabilities.

2.2.1 Software

Hector is an open-source community model available on GitHub (https://github.com/jgcri/hector). The repository includes updated project solutions and make files to support building and running Hector from the command line or IDEs such as Visual Studio and Xcode. Alternatively, users now have the option to run Hector as an R (R Core Team 2021) package (Dorheim et al. 2023). The scientific implementation of Hector in C++ was integrated with an R package wrapper using the Rcpp package (Eddelbuettel and Francois 2011). Thus, now users have the ability to build, run, and analyze Hector results in an R

https://doi.org/10.5194/egusphere-2023-1477
Preprint. Discussion started: 7 September 2023

environment, allowing for a broader range of users given R's popularity as a data analysis and simulation tool across many scientific disciplines. Furthermore, the R package wrapper enabled the development of a Shiny (https://shiny.rstudio.com/) application, the Hector User Interface (Hector UI) (Pennington and Vernon 2022), which allows users to run and interact with Hector results in a web browser. Other changes include updated and reduced software dependencies (it now depends only on Boost, https://www.boost.org/); expanded unit testing: and auto-generated online documentation. Ultimately these Hector V3 software changes have led to a more robust, transparent, and accessible community model. Additionally, a Python wrapper Pyhector (Willner et al. 2017) has been developed and maintained by community collaborators, broadening the potential users and use cases of the model.

2.2.2 Carbon Cycle

Hector's carbon cycle is split into the terrestrial land and ocean carbon cycle. As described in Hartin et al. (Hartin et al. 2015; Hartin et al. 2016), Hector's ocean carbon cycle is a four-box module, consisting of two surface-level, an intermediate, and a deep ocean boxes (Figure 1). Carbon and water mass exchange occur between the four boxes respecting simplified representations of advection and thermohaline circulation. Hector solves for the marine carbonate variables (i.g., DIC, pH, alkalinity,) with respect to solubility in the two surface layer boxes. Hector's V3 ocean carbon cycle now uses sea surface temperature (SST) calculated by DOECLIM and pre-industrial ocean carbon value from IPCC sixth assessment report (AR6) AR6 Figure 5.12 (Canadell et al. 2021b) to initialize Hector's ocean carbon pools.

Much of the basic functionality of the model's terrestrial carbon cycle is unchanged from the original V1 release described in Hartin et al. (2015). Net primary production (NPP) is partitioned into vegetation, detritus, and soil (Figure 1); litterfall moves carbon from vegetation to the soil, and temperature-dependent, first-order decay equations control the heterotrophic release of CO2 back to the atmosphere from the latter two pools (Hartin et al. 2015). By default, the terrestrial carbon cycle operates on a single, global biome, but this configuration can be changed: Hector can run with an arbitrary number of independent biomes, each with its own set of carbon pools and behavioral parameters, documented in detail in Woodard et al. (see e.g. Woodard et al. 2021).

There are, however, some new or changed behaviors in the Hector V3 terrestrial carbon submodel. Previously land use change (LUC) emissions were specified as a single time series that could be positive or negative, reflecting net emission or uptake; these are now provided in separate input time series that must be strictly positive and correspond to the gross emissions and uptake fluxes, respectively. A similar change has been made to the fossil fuel/industrial) emissions, which is now specified by two gross fluxes of emissions and uptake (e.g., through carbon capture and storage). This provides users with more flexibility to specify how the gross fluxes (uptake and emission) result in the net flux. Note that the model still accepts net fluxes if that is all that is available, as is the case for the RCMIP Shared Socioeconomic Pathway (SSP) scenarios (Nicholls et al. 2020).

https://doi.org/10.5194/egusphere-2023-1477
Preprint. Discussion started: 7 September 2023

Second, LUC fluxes now affect the land carbon pools in proportion to those pools' size, not via fixed allocation fractions as previously. This is a more conservative assumption and provides smoother, more intuitive model behavior under steady-state conditions. Third, NPP is now affected by LUC: the model tracks how much cumulative carbon has been lost (or gained) due to LUC, relative to preindustrial conditions, and then adjusts NPP by this fraction in addition to the pre-existing temperature and CO_2 adjustments to NPP described by Hartin et al. (2015). The new behavior is thus:

$$NPP(t) = NPP_0 f(C_{atm}, \beta) f(LUC_v) \quad (1)$$

where t is the current timestep; NPP0 is pre-industrial NPP; and the two f terms represent CO_2 fertilization (Wang et al. 2020) and the aforementioned LUC effect on NPP. This provides a better match with known LUC effects on terrestrial biomass and production (Winkler et al. 2021).

Hector V3 also includes a novel implementation of permafrost thaw, a potentially significant feedback affecting the earth system (Hugelius et al. 2020), that releases both CO_2 and CH_4 into the atmosphere. Hector's permafrost implementation was fully described by Woodard et al. (see e.g. 2021). Briefly, permafrost is treated as a separate land carbon pool that becomes available for decomposition into both CH_4 and CO_2 once thawed (Schädel et al. 2014). The thaw rate is controlled by biome-specific land surface temperature and calibrated to be consistent with both historical data and CMIP6 projections (Burke, Zhang, and Krinner 2020). Woodard et al. (2021) found that the fraction of thawed permafrost carbon available for decomposition was the most influential parameter in this scheme and that adding permafrost thaw to Hector resulted in 0.2–0.25 °C of additional warming over the 21st century. The permafrost functionality is not enabled by default in Hector V3, but is available for users if needed.

An additional new science feature in Hector V3 is the ability to track the flow of carbon (as CO_2) as it moves between the land and ocean carbon pools and the atmosphere. At a user-defined start-tracking date, the model tags all carbon in each of its pools as self-originating—e.g., the soil pool is deemed to be composed of 100% soil-origin carbon. As the model then runs forward, the origin tag is retained as carbon is exchanged between the models' various pools; if 1 Pg C with origin X are incorporated into a 19 Pg C pool with origin Y, for example, at the next timestep, the 20-Pg C pool is tracked as 5% origin X, 95% origin Y. At the end of a run, detailed information about the composition of each pool at each time point can be analyzed. This capability does not affect model behavior or any outputs, although it does impose a substantial performance penalty. This capability was described in detail by Pressburger et al. (2023) and is off by default because of its increased run time.

https://doi.org/10.5194/egusphere-2023-1477
Preprint. Discussion started: 7 September 2023

2.2.3 Radiative Forcing

At each time step after Hector's carbon cycle solves and all GHG concentrations are computed, then Hector calculates total radiative forcing. Hector's total radiative forcing is the sum of 39 forcing effects (listed in SI Table 1), each relative to the 1750 base year. The forcing effects for volcanoes, albedo, and "miscellaneous forcers" (by default, this is set to zero but can be used to read in additional forcing times series for a particular experiment protocol such as geoengineering, variation in solar radiation, black carbon on snow, and so on) are read in as inputs. The remaining 36 forcing effects for various aerosols, aerosol-cloud interactions, pollutants, and greenhouse gases are calculated internally within Hector. The forcing effects of tropospheric O3 and stratospheric H2O use the same calculations as Hartin et al. (2015). For the other forcing agents, CO_2, CH_4, N_2O, 26 halocarbons, aerosol-cloud interactions, and effects of BC, OC, SO_2, and NH_3, Hector V3 has adopted the forcing equations from AR6 (see supplement). Of these, the forcing effect from NH3 was not previously included in Hector. In addition, the aerosol-cloud interaction forcing replaces the indirect effects of SO2 forcing that was used to approximate the SO2 and cloud interactions in previous versions of Hector.

2.2.4 Temperature

As of V2, Hector replaced a 0-D energy balance model with DOECLIM (Vega-Westhoff et al. 2019). DOECLIM uses Hector's total radiative forcing to determine global temperature change. DOECLIM is a four-box energy balance model, meaning that it models heat transfer within the climate system represented by four idealized boxes: land (surface), air (troposphere) over land, air (troposphere) over the ocean, and sea surface (ocean mixed layer). DOECLIM uses a system of differential equations to model the temperature change in the four boxes in response to radiative forcing while accounting for the proportional differences in ocean and land masses and effective heat capacity (Kriegler 2005; Tanaka et al. 2007). The (Vega-Westhoff et al. 2019) implementation of Hector with DOECLIM was found to exhibit improved ocean heat uptake and temperature responses to radiative forcing.

In Hector V3, DOECLIM is a fully integrated component of the model, and its outputs now affect Hector's land carbon cycle (with DOECLIM's land temperature used to drive effects on heterotrophic respiration); similarly, sea surface temperature affects ocean carbon cycle dynamics. The difference in land and ocean temperature change, or land-ocean warming ratio, is an emergent property of DOECLIM and is used by default. However, a new Hector V3 feature allows users to prescribe a specified land-ocean warming ratio. This user-defined land-ocean warming ratio allows Hector users to better tune Hector model parameters to emulate a specific ESM behavior (see supplement). Two additional parameters, and , are scalar terms that can be used to adjust the contributions of aerosol (BC, OC, SO2, NH3, and aerosol-cloud interactions) and volcanic forcing to global temperature. By default and are set to a value of one, with the assumption being that the forcing-temperature relationship is consistent for all forces. These scalar terms allow users to adjust the temperature sensitivity to aerosol and

https://doi.org/10.5194/egusphere-2023-1477
Preprint. Discussion started: 7 September 2023

volcanic forcing in uncertainty analyses and or when using Hector to emulate ESMs that exhibit different sensitivities to aerosol and volcanic forcings (Dorheim et al. 2020).

2.2.5 Constraints

As mentioned previously, Hector can run in a constrained mode, which allows users to overwrite a specified Hector variable with a prescribed time series. Constraints such as CO_2 concentrations, global temperature anomaly, and total radiative forcing have been available since Hector's initial release. New constraints available in V3 include concentration constraints for all non-CO_2 GHGs and net biome production (NBP, effectively turning off the model's terrestrial carbon cycle). When running in the constrained mode, user-provided values seamlessly overwrite internally-calculated ones, and thus will be used by the downstream Hector components. For example, a Hector run that uses the total RF constraint will use the user-prescribed total RF time series to calculate energy fluxes and temperature change instead of Hector's internally calculated total RF (see Table 1 for more examples and details).

The ability to run in the constrained mode is a useful feature that has a number of applications, including the following three examples. For example, Hector's concentration constraints enable concentration-forced experiments (e.g., 1% CO2 and abrupt 4 x CO_2 (Eyring et al. 2016)) to comply with the RCMIP protocol (Nicholls et al. 2020). In addition, constraints facilitate coupling Hector with other models. The NBP constraint can be used to pass global NBP value from a regional terrestrial carbon cycle model to Hector, and from there, Hector's ocean carbon cycle and climate dynamics will be calculated. Finally, running Hector in constrained mode can help diagnose model behavior. Consider a situation where a new model development leads to an unexpected increase in global temperature. Running Hector with constrained CO_2 concentrations or with total RF will help the developer attribute this novel behavior to changes to Hector's carbon cycle or climate dynamics.

2.2.6 Model Parameterization

Hector's V3 default parameterization is mostly inherited from previous versions of Hector (Vega-Westhoff et al. 2019; Hartin et al. 2015), with the exception of when robust updated estimates are available. Hector V3 uses more recent estimates published for pre-industrial NPP, CO_2, CH_4, and N_2O concentrations, as well as estimates of the pre-industrial carbon cycle to initialize its ocean carbon pools (Table 2). Initial pre-industrial sea surface temperatures used by Hector's ocean component were updated from a CMIP5 multi-model mean to a CMIP6 multi-model mean. Historical ocean surface temperature output files from 24 CMIP6 participating models (see supplement Table 6) were processed to compute the area-weighted mean temperature globally, at high (> 55°), and at low latitudes (< 55°) from 1850 to 1860 (Table 2).

Five additional Hector parameters were fit to the comparison data using a Nelder-Mead optimization routine (Nelder and Mead 1965) in a two-part calibration protocol. First, the natural N_2O and CH_4 emissions, which are assumed to be constant throughout the run, were calibrated to median AR6 N_2O and CH_4 radiative forcing (Smith et al. 2021). Second, three Hector parameters—

https://doi.org/10.5194/egusphere-2023-1477
Preprint. Discussion started: 7 September 2023

CO2 fertilization factor β (unitless), heterotrophic respiration temperature sensitivity factor Q10 (unitless), and ocean heat diffusivity κ (cm2 s−1)—were fitted to historic CO2 concentrations (Dlugokencky, Tans, and Keeling 2018a) and global mean surface temperature (GMST) (Lenssen et al. 2019) observations. The optimization routine minimized the average of the two variables' mean squared errors between Hector CO_2 concentrations and observations (Dlugokencky, Tans, and Keeling 2018a) from 1959 to 2021 and Hector GMST anomaly (relative to 1950 to 1980) and observations (Lenssen et al. 2019) from 1880 to 2021. The best fits found for β, Q_{10}, and κ (Table 2) were then used as Hector's default parameters. The materials and scripts used to calibrate Hector are available in the manuscript repository (https://github.com/kdorheim/Dorheim_etal_2023_HectorV3) to ensure the reproducibility and transparency of the calibration process.

2.3 Model runs and analysis

All of the Hector V3 results included in the main body of this manuscript were generated using the model's default setup, with both the permafrost module and carbon tracking turned off. Unless otherwise specified, these results are from emission-driven inputs according to the RCMIP protocol for historical and future SSP scenarios (Nicholls et al., 2020, 2021) with the default parameterization described in the previous section.

To judge model performance we compared Hector results with both observations and ESM projections. No calibration data were subsequently used for validation. We used root mean squared error (RMSE) to quantify the differences between model results and the observations. An ordinary least squares linear regression was fit to Hector results and the observational data products to provide additional insights into the goodness of fit. An R2 value close to one suggests a high degree of correlation between the Hector results and the observations. Hector's GMST results from 1850 to 2021 were compared with HadCRUT5 (Morice et al. 2021) GMST observations, while Hector's CO_2 concentration results from 1750 to 1958 were compared with the CMIP6 (Malte Meinshausen et al. 2017) 2017 CO_2 concentrations. Because the (Meinshausen et al. 2017) CO_2 record is a synthesis of multiple observational datasets, including the (Dlugokencky, Tans, and Keeling 2018b) dataset (which was used to calibrate the historical portion of Hector's output), the comparison of Hector CO_2 concentrations with observations was limited to results from 1750 to 1958, thus excluding the portion of the (Meinshausen et al. 2017) record that was used in Hector's calibration to provide an out-of-sample RMSE value.

For the future period, we compared Hector's temperature with temperature results with ESM output made available via CMIP6. For this comparison, Hector was run in a *constrained mode*, in which concentrations for CO_2, CH_4, N_2O, and 26 halocarbons from RCMIP (Nicholls et al., 2020) were used to drive Hector. This is consistent with the CMIP6 protocol (Eyring et al., 2016), allowing for a direct comparison of Hector's climate dynamics with that of the ESMs. For this comparison, output files from 15 ESMs were processed to compute area-weighted global air, land air, and sea surface temperature anomaly. The CMIP6 models were selected based on data availability for the variables and scenarios; a complete list of models is given in the Supplementary Information (SI Table 8). Since higher-than-expected temperatures and climate sensitivity have been observed in many CMIP6 models (Zelinka et al., 2020), the ESM temperature results were categorized with respect to their equilibrium climate sensitivity (ECS) according to the IPCC AR6 assessed "very likely" range of 2-5 °C (Arias et al., 2021). ESMs with ECSs outside of that range were categorized as being "not very likely". Hector's projected near-term (2021-2024), mid-term (2041-2060), and long-term (2081-2100) warming was compared with the AR6 assessed values. Hector's warming was computed as the 20-year average global mean surface temperature, following the RCMIP emission-driven SSP protocols, whereas the AR6 assessed the best estimate, with "very likely" ranges determined using multiple lines of evidence (IPCC 2021).

For the future period, we compared Hector's temperature with temperature results with ESM output made available via CMIP6. For this comparison, Hector was run in a constrained mode, in which concentrations for CO_2, CH_4, N_2O, and 26 halocarbons from RCMIP (Nicholls et al. 2020) were used to drive Hector. This is consistent with the CMIP6 protocol (Eyring et al. 2016), allowing for a direct comparison of Hector's climate dynamics with that of the ESMs. For this comparison, output files from 15 ESMs were processed to compute area-weighted global air, land air, and sea surface temperature anomaly. The CMIP6 models were selected based on data availability for the variables and scenarios; a complete list of models is given in the Supplementary Information (SI Table 8). Since higher-than-expected temperatures and climate sensitivity have been observed in many CMIP6 models (Zelinka et al. 2020), the ESM temperature results were categorized with respect to their equilibrium climate sensitivity (ECS) according to the IPCC AR6 assessed "very likely" range of 2-5 °C (Arias et al. 2021). ESMs with ECSs outside of that range were categorized as being "not very likely". Hector's projected near-term (2021-2024), mid-term (2041-2060), and long-term (2081-2100) warming was compared with the AR6 assessed values. Hector's warming was computed as the 20-year average global mean surface temperature, following the RCMIP emission-driven SSP protocols, whereas the AR6 assessed the best estimate, with "very likely" ranges determined using multiple lines of evidence (IPCC 2021).

3 Results & Discussion

A crucial indicator for climate models is their ability to produce output consistent with historical and present-day observations. Figures 2 and 3 show such a comparison for Hector's CO_2 concentrations and GMST. Hector's historical CO_2 concentrations from an emission-driven run are compared with the Meinshausen et al. 2017 dataset in Figure 2. The Hector results closely follow the observed values with a RMSE of 2.63 ppm CO_2 between 1750 and 1958 (the portion of the available observations that was not used to calibrate Hector), with a correlation coefficient of 0.99 between Hector and observations. This small

https://doi.org/10.5194/egusphere-2023-1477
Preprint. Discussion started: 7 September 2023

RMSE and high correlation coefficient indicate a good agreement between Hector's output and historical carbon cycle observations.

Figure 3 compares emission-driven Hector GMST output with observations. The difference between Hector's results and observations is an RMSE of 0.16 °C, which is less than the standard deviation of the comparison dataset. The linear fit between Hector results and observations has an adjusted R2 value of 0.87 (Figure 3). The recent (2012-2021) decadal average global mean surface temperature for Hector was 0.99 ± 0.1 °C consistent with the 1 °C of historical warming observed in RCMIP Phase 1 (Z. R. Nicholls et al. 2020). The observed modern decadal average sea surface temperature, ocean pH, and NPP are 0.84 ± 0.08 °C, 8.1 ± 0.007, and 59.4 ± 0.27 Pg C/yr, respectively. Hector's land sink for 2012-2021 was 1.94 ± 0.093 Pg C/yr, which is lower than the land sink of 3.1 ± 0.6 PgC yr−1 reported by the Global Carbon Project (GCP) during the same decade. Despite that, Hector's ocean sink, 3.06 ± 0.14 Pg C/yr is consistent with the GCP ocean sink of 2.9 ± 0.4 PgC/yr. Ultimately emission-driven Hector historical results are in good agreement with observational records, which is an indicator of good climate model performance.

The comparison of Hector's historical results with observations is complemented by comparing Hector's future temperature results with CMIP6 results (Figure 4) and AR6 assessed warming (IPCC 2021). For the future SSP1-2.6, SSP2-4.5, and SSP5-8.5 projections, Hector's temperature results fall squarely within the CMIP6 ESM model spread (Figure 4). Hector's global mean air temperature and mean land surface temperature results for SSP1-2.6, SSP2-4.5, and SSP5-8.5, all fall within the spread of models belonging to the "very likely" category. Hector's sea surface temperature for SSP1-2.6, SSP2-4.5, and SSP5-8.5 projections fall along the cusp of the "very likely" ESM temperature range (Figure 4 right-most column). Furthermore, all of Hector's projected changes in global surface temperature were consistent with the assessed "very likely" range and less than 0.2 °C from the AR6 best estimate (SI Table 9).

Cumulative greenhouse gas emissions strongly influence global mean temperature, and the relationship between these two factors is an important metric for assessing both models and scenarios (Schwalm, Glendon, and Duffy 2020). Hector's relationship between global surface temperature and cumulative CO_2 emissions reveals a near-linear relationship (Figure 5) consistent with AR6 findings (Ipcc 2021), although the modeled historical temperature is slightly lower at ~1500 Pg C cumulative emissions, corresponding to the late 20th century. Per 1000 Pg of C, Hector's temperature increases by 2.0°C. While Hector's CO_2-temperature relation is warmer than the IPCC AR6 assessed best estimate of 1.65 °C per 1000 PgC, Hector's value does fall within the likely range of 1.0 to 2.3 °C per 1000 PgC (Arias et al. 2021).

4 Conclusions

In this manuscript, we documented the changes and new features of Hector V3. We showed that free-running Hector's historical results are generally consistent with observed CO_2 concentrations and global mean surface temperature, as well as historic warming produced by RCMIP-participating RCMs. Hector's future projections of global temperature are also consistent with a CMIP6 ensemble of models whose ECS is within the AR6 "very likely" range. Furthermore, Hector's projections fall within the AR6 assessed warming range for the various scenarios, a range that is based on multiple lines of evidence. Thus, we conclude that despite its relative simplicity, Hector is able to reproduce historical trends and 21st-century projections that are consistent with more complex climate models.

This fidelity to the current climate and future CMIP6 projections means that there are many potential use cases for Hector. Hector, including the online Hector UI, could be used in a classroom setting so that students can get hands-on experience with running a climate model and interpreting results; such educational use is supported by the fact that Hector is a well-documented open-source climate model with multiple means of running the model (Hector UI, R Hector, and C++ executable). The C++ executable can be coupled with other modeling tools, such as integrated assessment models, spatially resolved climate emulators, and so on. Using the Hector R package (Dorheim et al. 2023), it is easy to generate and analyze large ensembles of Hector results which can be used to explore uncertainty spaces (L. Pressburger et al. 2023; Z. Nicholls et al. 2021). Finally, Hector's performance and open, flexible calibration procedure mean that it has strong potential to emulate more-complex ESMs in support of novel, computationally-intensive experiments (Lu and Ricciuto 2019; Chen et al. 2023).

Despite the wide range of potential applications, it is important to note some of Hector's limitations. Hector currently underestimates the terrestrial carbon sink, which was also noted by (Pressburger et al. 2023) and may contribute to Hector's warmer end-of-century temperatures. Additionally, Hector does not account for the ocean biological pump or changes in ocean stratification; whether these errors are compensating or compounding is unclear and merits future research (Wan et al. 2013). Future work should aim at understanding/rectifying the differences between Hector's terrestrial carbon sink and other sources while remaining consistent with Hector moderate complexity and goals; it will always be important to consider trade-offs between costs (i.e., increased complexity threatening interpretability; increased predictive uncertainty from additional model parameters; computational efficiency) and benefits (increased fidelity and representativeness) (Sarofim et al. 2021).

In addition to continued science improvements, future versions of Hector will benefit from added infrastructure capabilities. First, the current parameter-calibration routine (described in §2.2.6 above) is relatively simple—for example, it does not consider uncertainty in the observational record—and it may be worth exploring more sophisticated model-calibration procedures (Chen et al. 2023) in future versions of Hector. Finally, a turnkey ability to do probabilistic model forecasts

(Fawcett et al. 2015; Ou et al. 2021), i.e. propagating parameter distributions and uncertainty (Pressburger et al. 2023) to produce probabilities of future climate change, is an important capability that will be addressed in the near future.

Code Availability: Specifically, Hector V3.1.1 was used to generate the Hector results analyzed and used to generate the figures included in the main text and in the supplementary information. This version of Hector is available at https://github.com/JGCRI/hector at the V3.1.1 release and is archived at https://zenodo.org/record/8306489 this includes all the initialization, emission, and concentration files. All of the code and data used to calibrate Hector as well as complete model runs and visualize results is available at https://github.com/kdorheim/Dorheim_etal_2023_GMD specifically the GMD2 release archived at https://zenodo.org/record/8306742.

Data Availability: All of the calibration, comparison data, and Hector results, along with scripts used to prepare Hector runs analyzed and used to generate the figures included in the main text and in the supplementary information, are available at https://github.com/kdorheim/Dorheim_etal_2023_GMD specfiCallly release GMD2 and archived at zendo https://zenodo.org/record/8306742.

Author contribution: KD, BB, SS, SK, RG, CH, LP, AS, and DW all contributed to Hector development. CT and SS helped conceptualize model experiments. KD and BB led the preparation of the original draft and all coauthors contributed to the final draft.

Competing interests: The authors declare that they have no conflict of interest.

Disclaimer: The views expressed in this article are those of the authors and do not necessarily represent the views or policies of the U.S. Department of Energy, Environmental Protection Agency, or National Aeronautics and Space Administration.

Acknowledgments: This research was supported by the U.S. Department of Energy, Office of Science, as part of research in MultiSector Dynamics, Earth and Environmental System Modeling Program. The authors would also like to acknowledge EPA Project DW-089-92459801-8 for contributing to the radiative forcing updates including in Hector v3. The authors would also like to acknowledge Robert Link and Sven Willner for their contributions to Hector and work on Rhector and Pyhector, respectively.

References

Arias, P. A., Bellouin, N., Coppola, E., Jones, R. G., Krinner, G., Marotzke, J., Naik, V., Palmer, M. D., Plattner, G.-K., Rogelj, J., Rojas, M., Sillmann, J., Storelvmo, T., Thorne, P. W., Trewin, B., Achuta Rao, K., Adhikary, B., Allan, R. P., Armour, K., Bala, G., Barimalala, R., Berger, S., Canadell, J. G., Cassou, C., Cherchi, A., Collins, W., Collins, W. D., Connors, S. L., Corti, S., Cruz, F., Dentener, F. J., Dereczynski, C., Di Luca, A., Diongue Niang, A., Doblas-Reyes, F. J., Dosio, A., Douville, H., Engelbrecht, F., Eyring, V., Fischer, E., Forster, P., Fox-Kemper, B., Fuglestvedt, J. S., Fyfe, J. C., Gillett, N. P., Goldfarb, L., Gorodetskaya, I., Gutierrez, J. M., Hamdi, R.,

https://doi.org/10.5194/egusphere-2023-1477
Preprint. Discussion started: 7 September 2023

Hawkins, E., Hewitt, H. T., Hope, P., Islam, A. S., Jones, C., Kaufman, D. S., Kopp, R. E., Kosaka, Y., Kossin, J., Krakovska, S., Lee, J.-Y., Li, J., Mauritsen, T., Maycock, T. K., Meinshausen, M., Min, S.-K., Monteiro, P. M. S., Ngo-Duc, T., Otto, F., Pinto, I., Pirani, A., Raghavan, K., Ranasinghe, R., Ruane, A. C., Ruiz, L., Sallée, J.-B., Samset, B. H., Sathyendranath, S., Seneviratne, S. I., Sörensson, A. A., Szopa, S., Takayabu, I., Tréguier, A.-M., van den Hurk, B., Vautard, R., von Schuckmann, K., Zaehle, S., Zhang, X., and Zickfeld, K.: Technical Summary, in: Climate Change 2021: The Physical Science Basis. Contribution of Working Group I to the Sixth Assessment Report of the Intergovernmental Panel on Climate Change, edited by: Masson-Delmotte, V., Zhai, P., Pirani, A., Connors, S. L., Péan, C., Berger, S., Caud, N., Chen, Y., Goldfarb, L., Gomis, M. I., Huang, M., Leitzell, K., Lonnoy, E., Matthews, J. B. R., Maycock, T. K., Waterfield, T., Yelekçi, O., Yu, R., and Zhou, B., Cambridge University Press, Cambridge, United Kingdom and New York, NY, USA, 33−144, 2021.

Calvin, K., Patel, P., Clarke, L., Asrar, G., Bond-Lamberty, B., Cui, R. Y., Di Vittorio, A., Dorheim, K., Edmonds, J., Hartin, C., Hejazi, M., Horowitz, R., Iyer, G., Kyle, P., Kim, S., Link, R., McJeon, H., Smith, S. J., Snyder, A., Waldhoff, S., and Wise, M.: GCAM v5.1: representing the linkages between energy, water, land, climate, and economic systems, Geoscientific Model Development, 12, 677–698, 2019a.

Calvin, K., Patel, P., Clarke, L., Asrar, G., Bond-Lamberty, B., Cui, R. Y., Vittorio, A. D., Dorheim, K., Edmonds, J., Hartin, C., and Others: GCAM v5. 1: representing the linkages between energy, water, land, climate, and economic systems, Geoscientific Model Development, 12, 677–698, 2019b.

Canadell, J. G., Monteiro, P. M. S., Costa, M. H., Cotrim da Cunha, L., Cox, P. M., Eliseev, A. V., Henson, S., Ishii, M., Jaccard, S., Koven, C., Lohila, A., Patra, P. K., Piao, S., Rogelj, J., Syampungani, S., Zaehle, S., and Zickfeld, K.: Global Carbon and other Biogeochemical Cycles and Feedbacks, in: Climate Change 2021: The Physical Science Basis. Contribution of Working Group I to the Sixth Assessment Report of the Intergovernmental Panel on Climate Change, edited by: Masson-Delmotte, V., Zhai, P., Pirani, A., Connors, S. L., Péan, C., Berger, S., Caud, N., Chen, Y., Goldfarb, L., Gomis, M. I., Huang, M., Leitzell, K., Lonnoy, E., Matthews, J. B. R., Maycock, T. K., Waterfield, T., Yelekçi, O., Yu, R., and Zhou, B., Cambridge University Press, Cambridge, United Kingdom and New York, NY, USA, 673–816, 2021.

Clarke, L.: Assessing Transformation Pathways, in: Climate Change 2014: Mitigation of Climate Change. Contribution of Working Group III to the Fifth Assessment Report of the Intergovernmental Panel on Climate Change, Cambridge University Press, 2014.

Dorheim, K., Link, R., Hartin, C., Kravitz, B., and Snyder, A.: Calibrating Simple Climate Models to Individual Earth System Models: Lessons Learned From Calibrating Hector, Life Support Biosph. Sci., 7, e2019EA000980, 2020.

Eyring, V., Bony, S., Meehl, G. A., Senior, C. A., Stevens, B., Stouffer, R. J., and Taylor, K. E.: Overview of the Coupled Model Intercomparison Project Phase 6 (CMIP6) experimental design and organization, Geosci. Model Dev., 9, 1937–1958, 2016.

Forster, P., Storelvmo, T., Armour, K., Collins, W., Dufresne, J.-L., Frame, D., Lunt, D. J., Mauritsen, T., Palmer, M. D., Watanabe, M., Wild, M., and Zhang, H.: The Earth's Energy Budget, Climate Feedbacks, and Climate Sensitivity, in: Climate Change 2021: The Physical Science Basis. Contribution of Working Group I to the Sixth Assessment Report of the Intergovernmental Panel on Climate Change, edited by: Masson-Delmotte, V., Zhai, P., Pirani, A., Connors, S. L., Péan, C., Berger, S., Caud, N., Chen, Y., Goldfarb, L., Gomis, M. I.,

https://doi.org/10.5194/egusphere-2023-1477
Preprint. Discussion started: 7 September 2023

Huang, M., Leitzell, K., Lonnoy, E., Matthews, J. B. R., Maycock, T. K., Waterfield, T., Yelekçi, O., Yu, R., and Zhou, B., Cambridge University Press, Cambridge, United Kingdom and New York, NY, USA, 923–1054, 2021.

Fuhrman, J., Bergero, C., Weber, M., Monteith, S., Wang, F. M., Clarens, A. F., Doney, S. C., Shobe, W., and McJeon, H.: Diverse carbon dioxide removal approaches could reduce impacts on the energy–water–land system, Nat. Clim. Chang., 13, 341–350, 2023.

Hartin, C., Patel, P., Schwarber, A., Link, R., and Bond-Lamberty, B.: A simple object-oriented and open-source model for scientific and policy analyses of the global climate system–Hector v1. 0, GMDA Bull., 939–955, 2015.

Hartin, C., Link, R., Patel, P., Mundra, A., Horowitz, R., Dorheim, K., and Clarke, L.: Integrated modeling of human-earth system interactions: An application of GCAM-fusion, Energy Econ., 103, 105566, 2021.

Hartin, C., McDuffie, E. E., Noiva, K., Sarofim, M., Parthum, B., Martinich, J., Barr, S., Neumann, J., Willwerth, J., and Fawcett, A.: Advancing the estimation of future climate impacts within the United States, EGUsphere, https://doi.org/10.5194/egusphere-2023-114, 2023.

Ipcc: Summary for Policymakers, in: Climate Change 2021: The Physical Science Basis. Contribution of Working Group I to the Sixth Assessment Report of the Intergovernmental Panel on Climate Change, edited by: Masson-Delmotte, V., Zhai, P., Pirani, A., Connors, S. L., Péan, C., Berger, S., Caud, N., Chen, Y., Goldfarb, L., Gomis, M. I., Huang, M., Leitzell, K., Lonnoy, E., Matthews, J. B. R., Maycock, T. K., Waterfield, T., Yelekçi, O., Yu, R., and Zhou, B., Cambridge University Press, Cambridge, United Kingdom and New York, NY, USA, 3−32, 2021.

Ito, A.: A historical meta-analysis of global terrestrial net primary productivity: Are estimates converging?, Glob. Chang. Biol., 17, 3161–3175, 2011.

Kawamiya, M., Hajima, T., Tachiiri, K., Watanabe, S., and Yokohata, T.: Two decades of Earth system modeling with an emphasis on Model for Interdisciplinary Research on Climate (MIROC), Progress in Earth and Planetary Science, 7, 1–13, 2020.

Kriegler, E.: Imprecise probability analysis for integrated assessment of climate change, Verlag nicht ermittelbar, 2005.

Meinshausen, M., Raper, S. C. B., and Wigley, T. M. L.: Emulating coupled atmosphere-ocean and carbon cycle models with a simpler model, MAGICC6 – Part 1: Model description and calibration, Atmos. Chem. Phys., 11, 1417–1456, 2011.

Nicholls, Z., Meinshausen, M., Lewis, J., Corradi, M. R., Dorheim, K., Gasser, T., Gieseke, R., Hope, A. P., Leach, N. J., McBride, L. A., Quilcaille, Y., Rogelj, J., Salawitch, R. J., Samset, B. H., Sandstad, M., Shiklomanov, A., Skeie, R. B., Smith, C. J., Smith, S. J., Su, X., Tsutsui, J., Vega-Westhoff, B., and Woodard, D. L.: Reduced Complexity Model Intercomparison Project Phase 2: Synthesizing Earth System Knowledge for Probabilistic Climate Projections, Earths Future, 9, e2020EF001900, 2021.

Nicholls, Z. R., Meinshausen, M., Lewis, J., Gieseke, R., Dommenget, D., Dorheim, K., Fan, C.-S., Fuglestvedt, J. S., Gasser, T., Golüke, U., and Others: Reduced complexity model intercomparison project phase 1: Protocol, results and initial observations, Geosci. Model Dev. Discuss, 2020.

Pressburger, L. and Dorheim, K. R.: JGCRI/hector_cmip6data: v1.0, https://doi.org/10.5281/zenodo.7304553, 2022.

https://doi.org/10.5194/egusphere-2023-1477
Preprint. Discussion started: 7 September 2023

Pressburger, L., Dorheim, K., Keenan, T., McJeon, H., Smith, S., and Bond-Lamberty, B.: Quantifying airborne fraction trends and the destination of anthropogenic CO2 by tracking carbon flows in a simple climate model, Environ. Res. Lett., in press, 2023.

Sarofim, M. C., Smith, J. B., St Juliana, A., and Hartin, C.: Improving reduced complexity model assessment and usability, Nat. Clim. Chang., 11, 1–3, 2021.

Schwarber, A. K., Smith, S. J., Hartin, C. A., Vega-Westhoff, B. A., and Sriver, R.: Evaluating climate emulation: fundamental impulse testing of simple climate models, Earth Syst. Dynam., 10, 729–739, 2019.

Smith, C., Nicholls, Z. R. J., Armour, K., Collins, W., Forster, P., Meinshausen, M., Palmer, M. D., and Watanabe, M.: The Earth's Energy Budget, Climate Feedbacks, and Climate Sensitivity Supplementary Material, in: Climate Change 2021: The Physical Science Basis. Contribution of Working Group I to the Sixth Assessment Report of the Intergovernmental Panel on Climate Change, edited by: Masson-Delmotte, V., Zhai, P., Pirani, A., Connors, S. L., Péan, C., Berger, S., Caud, N., Chen, Y., Goldfarb, L., Gomis, M. I., Huang, M., Leitzell, K., Lonnoy, E., Matthews, J. B. R., Maycock, T. K., Waterfield, T., Yelekçi, O., Yu, R., and Zhou, B., 2021.

Smith, C. J., Kramer, R. J., Myhre, G., Forster, P. M., Soden, B. J., Andrews, T., Boucher, O., Faluvegi, G., Fläschner, D., Hodnebrog, Ø., Kasoar, M., Kharin, V., Kirkev\aag, A., Lamarque, J.-F., Mülmenstädt, J., Olivié, D., Richardson, T., Samset, B. H., Shindell, D., Stier, P., Takemura, T., Voulgarakis, A., and Watson-Parris, D.: Understanding Rapid Adjustments to Diverse Forcing Agents, Geophys. Res. Lett., 45, 12,023–12,031, 2018.

Tanaka, K., Kriegler, E., Bruckner, T., Hooss, G., Knorr, W., Raddatz, T., and Tol, R.: Aggregated Carbon cycle, atmospheric chemistry and climate model (ACC2): description of forward and inverse mode, 2007.

Thornton, P. E. and Rosenbloom, N. A.: Ecosystem model spin-up: Estimating steady state conditions in a coupled terrestrial carbon and nitrogen cycle model, Ecol. Modell., 189, 25–48, 2005.

Vega-Westhoff, B., Sriver, R. L., Hartin, C. A., Wong, T. E., and Keller, K.: Impacts of observational constraints related to sea level on estimates of climate sensitivity, Earths Future, 7, 677–690, 2019.

Woodard, D. L., Shiklomanov, A. N., Kravitz, B., Hartin, C., and Bond-Lamberty, B.: A permafrost implementation in the simple carbon–climate model Hector v.2.3pf, Geosci. Model Dev., 14, 4751–4767, 2021.

Zelinka, M. D., Myers, T. A., McCoy, D. T., Po-Chedley, S., Caldwell, P. M., Ceppi, P., Klein, S. A., and Taylor, K. E.: Causes of higher climate sensitivity in CMIP6 models, Geophys. Res. Lett., 47, https://doi.org/10.1029/2019gl085782, 2020.

https://doi.org/10.5194/egusphere-2023-1477
Preprint. Discussion started: 7 September 2023

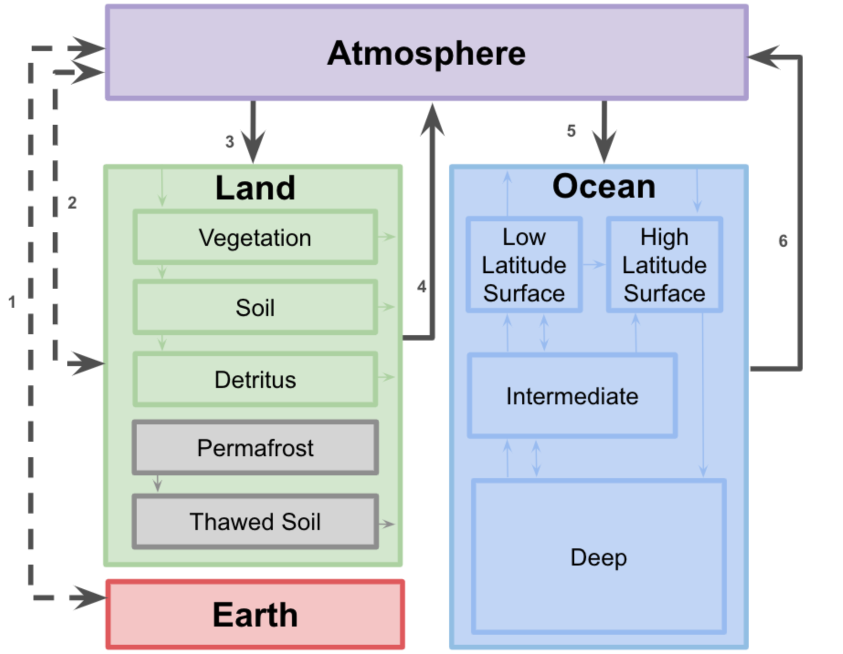

465

466 **Figure 1: Conceptual diagram of the CO_2 fluxes (numbered thick gray arrows) between Hector's four major carbon cycle boxes: a well-mixed atmosphere (Atmosphere), terrestrial carbon cycle (Land), ocean carbon cycle (Ocean), and fossil fuels (Earth). The thinner arrows within the land and ocean boxes allude to Hector's more complex submodule carbon cycle dynamics, which are not discussed in detail here. The solid lines indicate that CO_2 fluxes are calculated within Hector, whereas the dashed lines indicate that the fluxes are externally defined inputs read into the model. The fluxes are labelled: (1) CO_2 emissions from fossil fuels and industry and uptake carbon capture technologies; (2) CO_2 emissions and uptake from land use change (e.g., afforestation, deforestation, etc.); (3) vegetation uptake from the atmosphere (4) the aggregate CO_2 from respiration from the terrestrial biosphere; and ocean carbon (5) uptake and (6) outgassing. The model's permafrost implementation** (Woodard et al., 2021) **emits both CO_2 and CH_4 into the atmosphere, it is shown in gray because it is not enabled by default in the V3 model.**

475

476

Name	Description	Implementation
CO2_constrain	Time series of CO_2 concentration values (ppmv CO2)	CO_2 RF is calculated from the user-provided CO_2 concentrations and then used to calculate total RF and temperature. If needed, CO_2 is debited/credited to/from the deep ocean to meet the CO_2 concentration constraint and satisfy Hector's global carbon cycle mass balance check.
CH4_constrain	Time series of CH_4 concentration values (ppbv CH4)	CH_4 RF is calculated from the user-provided CH_4 concentrations, feeding into total RF and temperature.
N2O_constrain	Time series of N_2O concentration values (ppbv N2O)	N_2O RF is calculated from the user-provided N_2O concentrations.

https://doi.org/10.5194/egusphere-2023-1477
Preprint. Discussion started: 7 September 2023

X_constrain (X is the identifier for one of 26 halocarbons modeled by Hector)	Time series for a single halocarbon concentration (pptv)	RF for halocarbon X is calculated from the user-provided concentrations.
RF_tot_constrain	Time series of total radiative forcing value (W/m2)	User-provided total RF values are used to calculate temperature and heat flux. In this case, the emission inputs do not drive model behavior.
NBP_constrain	Time series of Net Biome Production values (Pg C/yr)	User-provided NBP values are used to up/downscale NPP and RH so that their total matches the constraint. This effectively bypasses the model's terrestrial carbon cycle.
tas_constrain	Time series of global mean air temperature values (°C)	User-provided temperature values overwrite Hector's, with a smooth transition between the constrained and free-running behavior.

Table 1: Descriptions and summaries of the implementation of the Hector constraints. The constraint name column reflects the name as it appears in the model's ini (initialization) files.

Parameter	**Description**	**Value**	**Units**	**Source**
CH4N	Natural CH4 Emissions assumed to be constant of the historical and future period	338	Tg CH4/yr	Calibrated to historical data see manuscript github repository
N2ON	Natural N2O emissions, assumed to be constant of the historical and future period	9.7	Tg N/yr	
beta	CO_2 fertilization factor (increase in NPP productivity with increasing CO_2 concentrations)	0.55	unitless	
q10_rh	Heterotrophic respiration temperature sensitivity factor	2.2	unitless	
diff	Vertical ocean heat diffusivity (κ), the rate of heat diffuses into the ocean	1.16	cm2/s	
preind_surface_c	Initial size of the preindustrial surface ocean carbon pool	900	Pg C	Figure 5.12 (Canadell et al., 2021)
preind_interdeep_c	Initial size of the preindustrial intermediate and deep ocean carbon pool	37100	Pg C	Figure 5.12 (Canadell et al., 2021)
C0	Preindustrial CO_2 concentration	277.15	ppmv CO2	Table 7.SM.1 (Smith et al., 2021)
N0	Preindustrial N_2O concentration	273.87	ppbv N2O	Table 7.SM.1 (Smith et al., 2021)
M0	Preindustrial CH_4 concentration	731.41	ppbv CH4	Table 7.SM.1 (Smith et al., 2021)

https://doi.org/10.5194/egusphere-2023-1477
Preprint. Discussion started: 7 September 2023

npp_flux0	Preindustrial net primary production	56.2	Pg C/yr	(Ito, 2011)
TOS0	Mean preindustrial absolute ocean air temperature	18	C	From processed CMIP6 data (Pressburger and Dorheim, 2022)
deltaHL0	Difference between high latitude preindustrial ocean temp and TOS0	-16.4	C	
deltaLL0	Difference between low latitude preindustrial ocean temp and TOS0	2.9	C	

Table 2: Default Hector parameter values and their sources. The parameter name column is the name as it appears in the model's ini (initialization) files. This is not an exhaustive table of Hector parameters but rather contains the parameters that have been updated since (Corrine Hartin et al. 2015). For a complete collection of parameter values and their sources, refer to the default ini files available at https://github.com/JGCRI/hector/tree/master/inst/input. Preindustrial values here are circa 1745, the start of a Hector run.

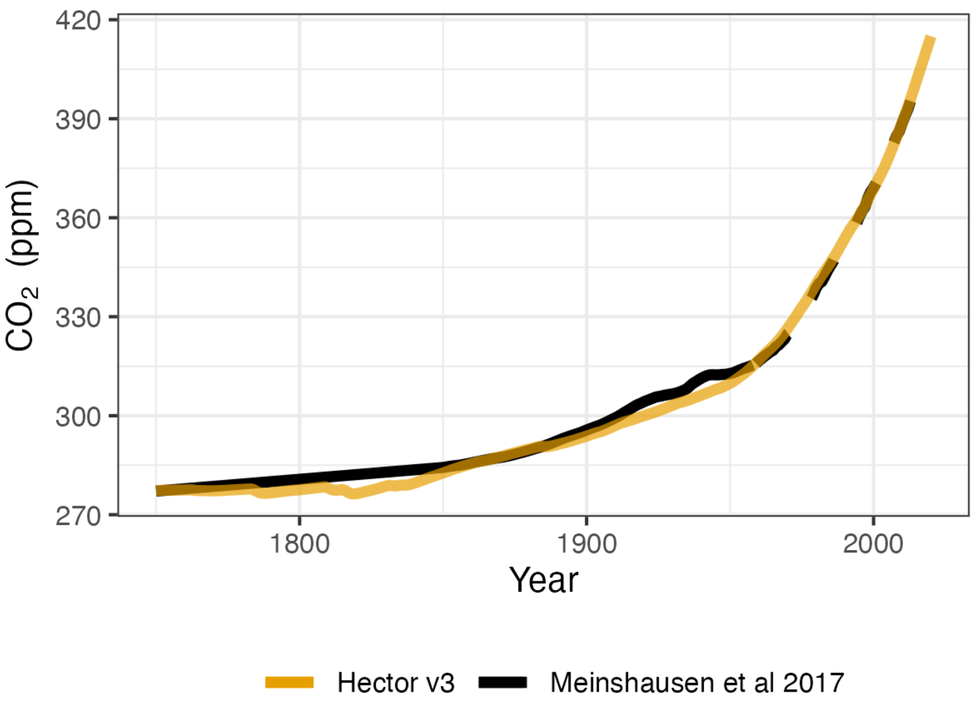

Figure 2: Hector CO2 concentrations (orange) compared with the CMIP6 (Malte Meinshausen et al. 2017) CO2 concentrations observational product (black). The dashed black line (1959-2014) represents the portion of the (Malte Meinshausen et al. 2017) record that was excluded from the Hector historical evaluation because it was used in the model calibration phase.

https://doi.org/10.5194/egusphere-2023-1477
Preprint. Discussion started: 7 September 2023

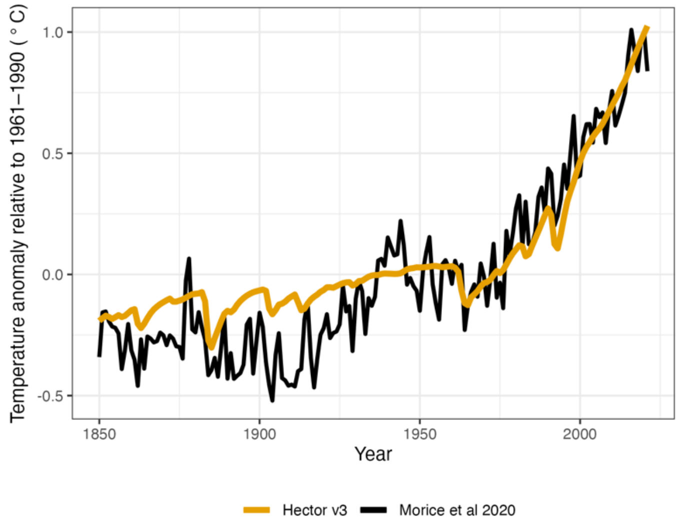

Figure 3: Global mean surface temperature anomaly relative to 1951-1980 for Hector (orange) and HadCRUT 5 global mean surface temperature observations (Morice et al. 2021) (black).

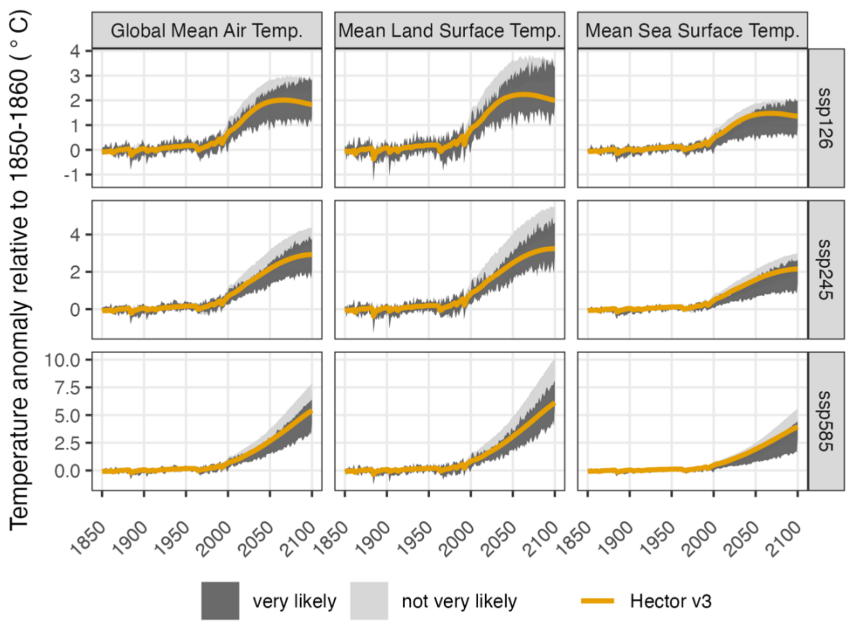

Figure 4: Temperature anomaly for GHG concentration from constrained Hector (orange) and the spread of 15 CMIP6 models. CMIP6 results are categorized according to their equilibrium climate sensitivity (ECS) according to the IPCC AR6 "very likely" range for ECS 2 to 5 °C (Arias et al. 2021) categorized as "not very likely".

https://doi.org/10.5194/egusphere-2023-1477
Preprint. Discussion started: 7 September 2023

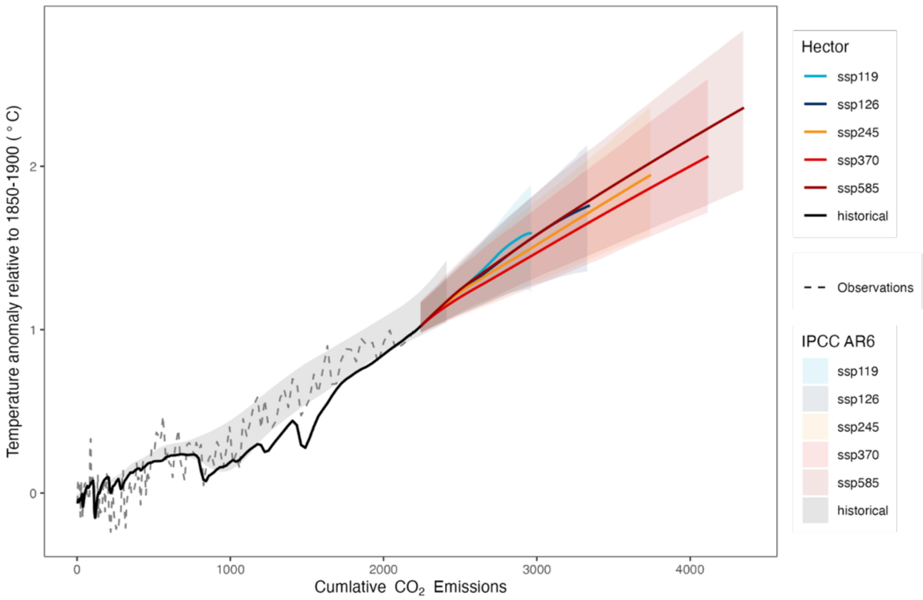

Figure 5: Recreated figure SPM10 from IPCC AR6: cumulative CO2 emissions versus temperature change relative to the 1850-1900 reference period. Hector's results are indicated by the thick solid lines, colored according to the scenario. Colored envelopes show IPCC AR6 uncertainty bounds. Observations are indicated by the dashed line. Note that Hector's historical land use emissions were updated so that cumulative Hector and AR6 total CO2 emissions were identical.